Comprehensive Model for Thermopneumatic Actuators and Microvalves

Albert K. Henning, *Member, IEEE*

***Abstract*—Thermopneumatic actuators have been used in a variety of microelectromechanical systems (MEMS) applications, particularly in the area of microvalves. However, a relatively simple model which relates the steady-state and transient response of the actuator to all important structural and boundary conditions has been lacking. In this work, a comprehensive model for thermopneumatic actuation is presented. The full thermodynamic nature of the thermopneumatic control fluid is modeled, including the change of phase from liquid, to liquid-vapor, to vapor, and back again. The thermodynamic model is coupled thermally and mechanically to a silicon membrane microstructure. The steady-state and transient response of the full actuator is modeled successfully, as represented by the application of the model to several modalities of interest. These include steady-state, isothermal flow of a compressible gas in a normally closed microvalve, and transient, nonisothermal flow in a normally open microvalve. This paper finishes with a discussion of the relevant assumptions in the model, the validity of the assumptions, and how departures from these assumptions can be assessed. [1460]**

***Index Terms*—Coupled mechanical, fluid mechanical modeling, lumped element system modeling, microfluidics, microvalve, thermal, thermopneumatic microactuators.**

NOMENCLATURE

T_{py1}, T_{py2}, $T_{Si}T_{FC}$, $T_{\rm mem}$, $T_{\rm pkg}$	State variables for model (K or °C).
$T_{\rm res}$, $T_{\rm amb}$	Temperature boundary conditions (K or °C).
R_{py1}, R_{py2}, R_{py3}, R_{FC1}, R_{FC2}, $R_{\rm mem}R_{Si}$, $R_{\rm pkg}$	Thermal resistivities for model (K/W).
C_{py}, C_{FC}, C_{Si}, $C_{\rm pkg}$	Specific heats for model (J/kg-K).
κ_{py}, κ_{FC}, κ_{Si}, $\kappa_{\rm pkg}$	Thermal conductivities for model (W/m-K).
ρ_{py}, ρ_{FC}, ρ_{Si}, $\rho_{\rm pkg}$	Densities for thermal model (kg/m^3).
$\rho_{\rm liq}$, $\rho_{\rm vap}$	Densities for thermopneumatic fluid model (kg/m^3).
$V_{\rm liq}$, $V_{\rm vap}$	Volumes for thermopneumatic fluid model (kg/m^3).
a	Length of square membrane side (m).
w_b	Bond width (for either anodic bond, or fusion bond) (m).
t_{py}, $t_{\rm mem}$, $t_{\rm cav}$, t_{Si}	Material thicknesses used in model (m).
δV	Volumetric change of hermetic cavity (m^3).
V_0	Initial volume of hermetic cavity (m^3).
η_f	Fraction of hermetic cavity filled by liquid during fill process (m^3).
$P_{\rm in}$	NO valve inlet pressure under flow conditions (Pa).
$P_{\rm out}$	NO valve outlet pressure under flow conditions (Pa).
$P_{\rm trans}$	Transmembrane pressure (Pa).
$P_{\rm cav}$	Thermopneumatic cavity pressure (Pa).
P_a	Ambient pressure (Pa).
$P_{\rm sat}$	Saturation pressure of thermopneumatic fluid (Pa).
M_f	Mass of thermopneumatic fluid sealed in hermetic cavity (kg).
A_s, B_s	Square membrane deflection coefficients (dimensionless).
A, B, C, D	Coefficients associated with Fluorinert liquids.
η_V	Ratio of $\delta V/a^2 s (0 < \eta_V \leq 1)$.
T_f	Temperature during cavity fill process (K).
s	Membrane stroke (m).
$s_{\rm boss}$	Displacement of the membrane boss due to membrane stroke (m).
λ, x_0, h_b, $t_{\rm puck}$, Δ	Dimensions associated with deflection of shutoff valve cantilever (m).
θ	Angle associated with deflection of shutoff valve cantilever (rad).
C_p	Gas specific heat at constant pressure (J/kg-K).
C_v	Gas specific heat at constant volume (J/kg-K).
γ	Ratio of C_p/C_v (dimensionless).
$\alpha(\gamma)$	Sonic flow factor (dimensionless).
$\delta(\gamma)$	Subsonic flow factor (dimensionless).
C_d	Coefficient of discharge (dimensionless).

Manuscript received November 5, 2004; revised February 25, 2006. Subject Editor Y.-C. Tai.

The author was with Redwood Microsystems, Inc., Menlo Park, CA 94025 USA. He is now with Aquarian Microsystems, Palo Alto, CA 94303 USA (e-mail: henning@aquarianmicro.com).

Digital Object Identifier 10.1109/JMEMS.2006.879665

A_{flow}	Effective flow area associated with microvalve flow model (m^2).
D_{inlet}	Inlet diameter of the NO microvalve (m).
gap_0	Flow gap when stroke is zero in normally-open valve (m).
gap, gap_{flow}	Gap parameters associated with flow in shutoff valve (m).
τ_{heater}	Time constant to heat/cool the Pt resistor (s).
h_{conv}	Convective heat transfer coupling coefficient (W/K).
R	Gas constant for flow model (J/kg-K).
R_{vap}	Gas constant for thermopneumatic fluid model (J/kg-K).

I. Introduction

THERMOPNEUMATIC microvalves have been studied for approximately twenty years. Initial investigations established the general principles of a rigid cavity, having one side bounded by a flexible membrane, and containing a heat source and a fluid. The fluid could have liquid-only, gas-only, and liquid-gas (mixed) thermodynamic phases. Changes between thermodynamic phases were also considered [1]–[4].

Subsequent work explored: liquid-to-gas phase change in greater detail [5]–[7]; low-power thermopneumatic microvalves [8], [9]; thermopneumatic actuators with highly flexible membranes from rubber or parylene [10], [11]; surface micromachined thermopneumatic actuators using paraffin as the cavity fluid [12]; and integrated thermopneumatic microvalves utilizing a corrugated membrane [13].

Published modeling work in this area has, however, been limited [2], [13], [14]. A quantitative, compact model which couples steady-state and transient flow to all important manufacturing and design parameters, and to all essential boundary conditions of temperature, pressure, and energy (power) input, is lacking entirely. It is the goal of this work to provide exactly such a model.

Unless otherwise noted, units employed for all model parameters are SI (MKS). Symbols and variables are defined in an Nomenclature.

II. Initial Thermodynamic State

To begin, the comprehensive model requires an accurate treatment of the thermodynamic behavior of the actuation fluid, as well as coupling to the mechanical output of the actuator. Satisfying these requirements establishes the initial thermodynamic state of the actuator.

Fig. 1 shows a schematic of a thermopneumatic actuator. The cavity is bounded rigidly on all sides, except for the side comprised of a flexible membrane. The cavity volume is V_0. Deflections of the membrane center cause a center displacement s, and an addition to the overall volume of δV.

If the central cavity is filled with a fluid, then the following assumptions guide the establishment of a quantitative thermodynamic state for the device, essential for either steady-state or transient modeling.

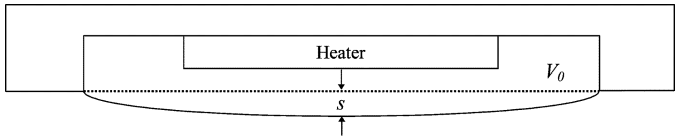

Fig. 1. Schematic of a thermopneumatic actuator.

- The membrane center deflection is a function of the change in hermetic cavity volume. This function may be nonlinear, but is monotonic.
- The cavity is isobaric under the fill conditions (the conditions of pressure and temperature wherein the fluid is introduced into the cavity), and under any subsequent operation conditions (pressure and temperature) of the actuator.
- The external pressure load on the membrane is uniform.
- The cavity is isothermal under the fill conditions.
- The cavity fluid in its vapor phase obeys the ideal gas law.

For most membranes—square, rectangular, or circular, with or without initial tension, with or without a central boss—the relationship between the membrane's center deflection s and the transmembrane pressure is described by [15]

$$\frac{P_{\text{trans}}a^4}{Eh^4} = A_s\frac{s}{h} + B_s\frac{s^3}{h^3}. \tag{1}$$

The membrane thickness h, its lateral extent a, and Young's modulus E are the principal structural and materials properties in this expression. The coefficients A_s and B_s also may have some material dependence, as reflected by Poisson's ratio [15]. Initial tension in the membrane may also be embedded in the coefficient B_s [16]. The effect of a rigid boss in the central portion of the membrane can also be reflected in these coefficients, but does not change the essential linear-cubic nature of the mechanical response to the transmembrane pressure [15].

This expression holds generally for a circular or rectangular membrane: Only the coefficients of the linear and cubic terms need to be altered. More complicated structures, such as corrugated membranes, require a different functional dependence relating the energy stored in the membrane to its displacement.

It remains to relate the change in the (hermetic) cavity volume to the transmembrane pressure. This volume change is described by

$$\delta V(P_{\text{trans}}) = \eta_V a^2 s(P_{\text{trans}}) \tag{2}$$

where s is found using (1), and $0 < \eta_V \leq 1$. A value of 1 for η_V corresponds to a pillbox deformation with either a square or round base. A value of 0.25 corresponds to a pyramidal deformation with a square base. A value of about 0.38 corresponds to small-deflection spherical deformation with a circular edge. In practical membranes—where the base is, for example, 4.2 mm square, and the thickness is 50 μm—the deformation transforms from a square shape near the membrane edge, to a circular shape as one approaches the membrane center. Values of the volume expansion factor η_V then should lie between 0.25–0.38 and are typically 0.345. Note also that for a square membrane, η_V may not be a constant of the center deflection s. That is, the volume expansion factor increases as the center deflection increases, reflecting the increasing stiffness in the membrane as it distends.

As a consequence, (1) and (2) must be altered substantially if balloon membranes [10] are to be modeled.

The liquid is introduced into the hermetic cavity under conditions of fill temperature and fill pressure. For the thermopneumatic microvalves of [1]–[4], [7]–[9], and [19], the fluids are chosen from the family of Fluorinert liquids [17], primarily for their large coefficient of thermal expansion, and their thermal and electronic stability. Note that other liquids have been explored in detail [2]. The density of the liquid sealed into the hermetic cavity is taken to be incompressible and given by

$$\rho_{\mathrm{liq}}(T) = 1000 \cdot \{C - D \cdot [T - 273]\}. \tag{3}$$

The coefficients C and D are found in [17]. However, for most of this work, a constant value will be used for a particular liquid, since the density varies by less than 10% over the expected range of Fluorinert temperatures in thermopneumatic applications.

The vapor density is given by the ideal gas law

$$\rho_{\mathrm{vap}}(P,T) = \frac{P}{R_{\mathrm{vap}}T}. \tag{4}$$

The gas constant R_{vap} is given by the universal gas constant, divided by the molecular weight for the particular Fluorinert. P in this instance is the (isobaric) cavity pressure.

Using these densities, and the volume parameters developed previously, the total mass sealed into the hermetic cavity is given by (5)

$$\begin{aligned} M_f(&P_{\mathrm{cav,fill}} - P_{a,\mathrm{fill}}, T_f) \\ &= [V_0 + \delta V(P_{\mathrm{cav,fill}} - P_{a,\mathrm{fill}})] \\ &\quad \times \{\eta_f \rho_{\mathrm{liq}}(T_f) + (1-\eta_f)\rho_{\mathrm{vap}}(P_{\mathrm{cav,fill}}, T_f)\} \\ &= [V_0 + \delta V(P_{\mathrm{cav,fill}} - P_{a,\mathrm{fill}})] \\ &\quad \times \left\{\eta_f \rho_{\mathrm{liq}}(T_f) + (1-\eta_f)\frac{P_{\mathrm{cav,fill}}}{R_{\mathrm{vap}}T_f}\right\}. \end{aligned} \tag{5}$$

The function δV is found through the use of (1) and (2). The fill factor η_f is the fraction of the initial cavity volume which is filled with liquid during the fill operation. Equation (5) says that the mass encapsulated in the hermetic cavity is equal to the cavity volume (determined by the manufactured volume, plus any changes caused by transmembrane pressure during the fill process), times the sum of (the liquid volume fraction times the liquid density, plus the vapor volume fraction times the vapor density).

III. Isothermal Operation Regimes

Having established the initial thermodynamic state in the hermetic cavity by relating the encapsulated mass to the various structural and thermodynamic parameters involved in the fill process, we turn our attention to the operation of the actuator under conditions of constant temperature. There are four regimes of operation: vapor-and-liquid phase due to cavitation; liquid-only phase; vapor-and-liquid phase due to evaporation; and vapor-only phase. These regimes may be understood in light of Fig. 2. In particular, the important distinction between a vapor-liquid regime due to cavitation, and one due to evaporation, is articulated.

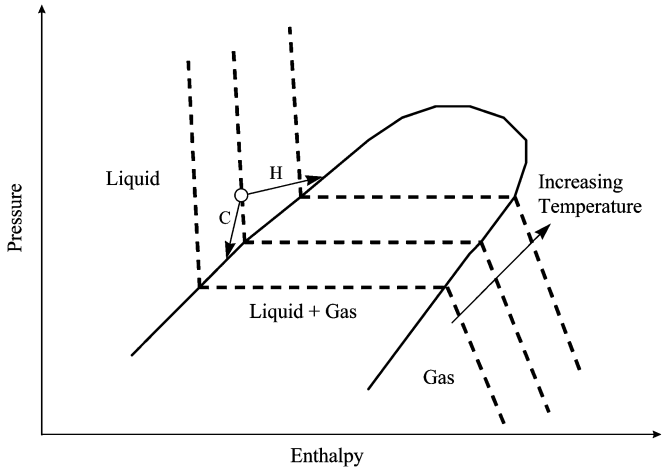

Fig. 2. Thermodynamic $P - h$ diagram for the control fluid in a thermopneumatic actuator. Dashed lines indicate isotherms. The typical, initial fill state is shown as a white circle. As the system cools, the thermopneumatic fluid follows the path "C." Once the vapor dome is crossed, two phases exist (due to cavitation), and the pressure in the cavity is set by the saturation temperature located (spatially) between the gas and liquid phases. Alternatively, as the system heats, the fluid follows the path "H." When the vapor dome is crossed, two phases exist (due to evaporation, or boiling), and again the pressure is set by the saturation temperature at the spatial location between the two phases. Prior to crossing the vapor dome, the pressure is set solely by the incompressible liquid.

The range of temperatures for the vapor-only phase requires cavity pressures which exceed the yield strength of our silicon membranes, presuming fill factors near unity, and so will not be evaluated. Analytically, however, it is a simple matter to include this regime.

For any isothermal temperature, both the saturation pressure and the "liquid" pressure are evaluated independently. The cavity pressure and the regime of operation are determined by whichever of these pressures is the greater.

For the Fluorinert liquids considered in this work, the saturation pressure in the isothermal and isobaric hermetic cavity is given by

$$P_{\mathrm{sat}}(T) = \frac{101356}{760} \cdot 10^{A - B/T}. \tag{6}$$

The coefficients A and B are found in [17]. The scaling factor which precedes the exponential converts the pressure from Torr to Pa.

In terms of a "liquid" pressure, assuming the cavity (at a given membrane deflection) contains only liquid, then the following expression is true:

$$\frac{M_f}{\rho_{\mathrm{liq}}(T)} = V_0 + \delta V(P_{\mathrm{cav}} - P_a). \tag{7}$$

This expression, when solved in conjunction with (1) and (2), allows the "liquid" pressure to be determined.

The mass encapsulated at the time of fill is a conserved quantity (provided, of course, there are no cavity leaks).

If the pressure calculated from (6) exceeds the pressure determined from (7), then the actuator cavity is in the vapor-liquid regime, where the cavity pressure is determined by the saturation pressure at the interface between the vapor and the liquid. In this regime, it is important to determine how much of the cavity

volume contains liquid, and how much contains vapor. This result can be found by first writing the mass conservation equation

$$M_f = \rho_{\text{liq}}(T) \cdot V_{\text{liq}} + \rho_{\text{vap}}(P_{\text{sat}}, T) \cdot V_{\text{vap}}. \tag{8}$$

The "conservation of volume" also requires that the total mechanical volume equals the total thermodynamic fluid volume

$$V_0 + \delta V(P_{\text{sat}} - P_a) = V_{\text{liq}} + V_{\text{vap}}. \tag{9}$$

Simultaneous solution of (8) and (9) yields

$$V_{\text{vap}}(P_a, T) = \frac{\rho_{\text{liq}}(T) \cdot [V_0 + \delta V(P_{\text{sat}} - P_a)] - M_f}{\rho_{\text{liq}}(T) - \rho_{\text{vap}}(P_{\text{sat}}, T)} \tag{10}$$

$$V_{\text{liq}}(P_a, T) = \frac{M_f - \rho_{\text{vap}}(P_{\text{sat}}, T) \cdot [V_0 + \delta V(P_{\text{sat}} - P_a)]}{\rho_{\text{liq}}(T) - \rho_{\text{vap}}(P_{\text{sat}}, T)}. \tag{11}$$

Equations (1)–(11) complete the quantitative description of a thermopneumatic actuator, in an isothermal environment, with an ambient pressure impinging on one side of the actuator cavity membrane. Nonisothermal operating conditions will be treated later.

Only (3) and (6) are specific to Fluorinert liquids. Other liquids can be described by their respective equations for liquid density and saturation pressure. Departures from the ideal gas law of (4) can be accommodated by use of alternative equations of state (EOS), such as the Redlich–Kwong EOS [18], for the thermopneumatic fluid.

A correction to these equations can be added, to account for the effect of cavity liquid surface tension on the inner face of the membrane, under cavitation conditions. This correction will be discussed in a subsequent work.

IV. Steady-State Isothermal Flow in a Normally Closed Thermopneumatic Microvalve

With the mechanical motion of the membrane now completely defined—in terms of the fill conditions, the membrane structural dimensions, the ambient (valve inlet) pressure, and the isothermal temperature—we can relate the membrane position to the valve flow. Fig. 3 defines several required parameters in order to do so for a vacuum leak rate shutoff microvalve, or SOV [19].

Using Fig. 3, the following relationships can be derived:

$$\begin{aligned} s_{\text{boss}} &= s \cdot \left(1 - \frac{2\lambda}{a}\right) \\ \theta &= \tan^{-1}\left(\frac{2s}{a}\right) \\ x_0 &= \frac{a}{2} - \lambda - h_b \sin\theta - (s_{\text{boss}} + h_b \cos\theta - h_b) \cdot \frac{a}{2s} \\ \text{gap} &= (\Delta - x_0)\tan\theta. \end{aligned} \tag{12}$$

To account for the thickness of the puck t_{puck} in the SOV cantilever, the gap which controls the flow must be less than the gap as shown in Fig. 3

$$\text{gap}_{\text{flow}} = \text{gap} - t_{\text{puck}}. \tag{13}$$

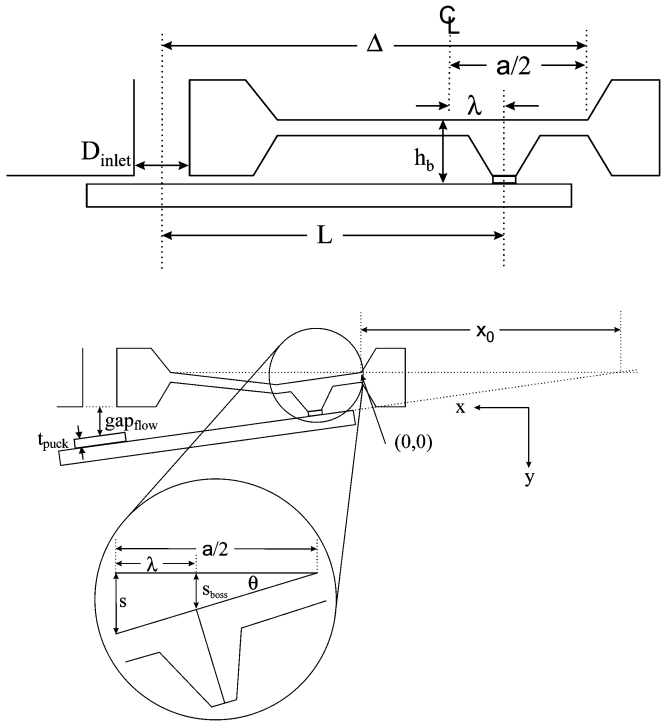

Fig. 3. Detailed schematics of a normally closed, thermopneumatically actuated shutoff microvalve (after [19]), including model parameters coupling valve structural and actuation parameters to those parameters important for modeling flow. Top: Valve in closed condition. Bottom: Valve in open condition. The parameters important directly to flow are D_{inlet} and gap_{flow}.

Finally, the sonic and subsonic mass flow rate equations, describing the compressible gas flow through the overall structure, are given by [20]

$$\begin{aligned} \dot{m}_{\text{subsonic}} &= \frac{P_{in}}{\sqrt{RT}} C_d A_{\text{flow}} \left(\frac{P_{\text{out}}}{P_{\text{in}}}\right)^{(\gamma+1/2\gamma)} \\ &\quad \times \delta(\gamma)\sqrt{\left(\frac{P_{\text{in}}}{P_{\text{out}}}\right)^{(\gamma-1/\gamma)} - 1} \\ \dot{m}_{\text{sonic}} &= \frac{P_{in}}{\sqrt{RT}} C_d A_{\text{flow}} \alpha(\gamma) \\ \alpha(\gamma) &= \sqrt{\gamma\left(\frac{2}{1+\gamma}\right)^{(\gamma+1/\gamma-1)}} \\ \delta(\gamma) &= \sqrt{\frac{2\gamma}{\gamma+1}} \\ \sqrt{A_{\text{flow}}} &= \left\{1 - \exp\left[-\frac{\frac{\text{gap}_{\text{flow}}}{D_{\text{inlet}}}}{0.068}\right]\right\}. \end{aligned} \tag{14}$$

Note that R is, in this instance, the gas constant for the gas being controlled, not the Fluorinert vapor. Note also that gap_{flow} is constrained to be zero or greater.

Note that the effective area for flow, A_{flow}, becomes modified, if the valve inlet is not a simple rectangle or circle, but takes on a complex perimeter structure [22].

This treatment completes the isothermal flow model. It remains to show its applicability in real devices. Fig. 4 shows a series of relatively complex examples. Here, the isothermal flows of a variety of SOVs are measured and modeled. The SOV

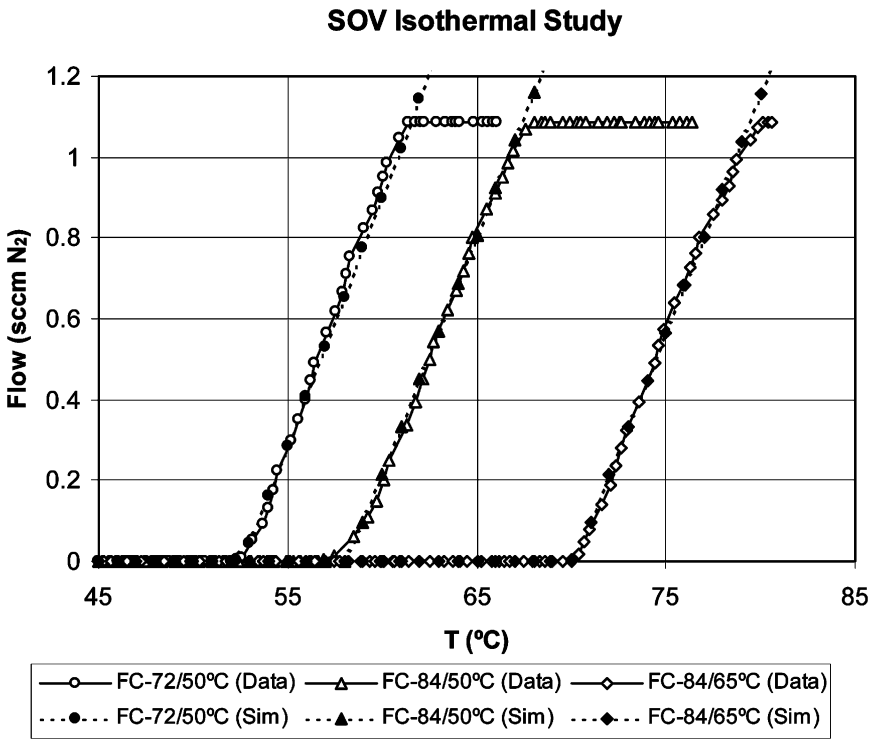

Fig. 4. Measured and simulated flow versus isothermal temperature for several normally closed shutoff valves. The measured plateaus at ~ 1.1 slm of flow are due to the saturation of the flow meter.

thermopneumatic cavities have been filled under the conditions noted in the figure caption. All model parameters are identical to the parameters measured or used in the manufactured device.

V. Transient Nonisothermal Flow in a Normally Opened Thermopneumatic Microvalve

The previous sections laid out the initial thermodynamic state of a thermopneumatic actuator, and its application to the prediction of steady-state flow in microvalves under isothermal conditions. In this section, the model is extended to cover transient microvalve flow, where the thermal boundary conditions are not uniform (i.e., where thermal power is delivered to the heater depicted in Fig. 1). This extension is accomplished through the addition of several features: a lumped element thermal model of the valve and package; convective heat transfer between the valve membrane and the gas stream; and the nonlinear (nonsimultaneous) fashion in which the membrane makes contact with the valve seat, especially when the valve seat area is large (for a single inlet orifice), or when it consists of an array of inlets [20], [22].

The use of a lumped element thermal model for the microvalve assumes atomic-level thermal processes reach a steady-state with a time constant small compared to the important system time constants. Although this system is a microvalve, nonetheless its dimensions are still large enough so that this important assumption remains valid.

To simplify the analysis somewhat in this section, we restrict the model to the liquid-only operating regime in the thermopneumatic actuator. A treatment of the actuator covering all operating conditions, under nonisothermal conditions, has been given elsewhere [7]. The simplification results in the following equations. The volumetric change is now related to the mean liquid temperature in the thermopneumatic actuator cavity

$$\delta V = V_0 \beta (T_{FC} - T_f). \tag{15}$$

Here, T_{FC} is the mean cavity liquid temperature, and β is the liquid's coefficient of thermal expansion. Since, for a circular or square membrane $V_0 = t_{\rm cav} a^2$ the relationship between s and T_{FC} is linear and straightforward

$$s = \frac{t_{\rm cav}\beta}{\eta_V}(T_{FC} - T_f). \tag{16}$$

The goal of the thermal model is thus to extract the mean temperature of the liquid in the thermopneumatic actuator cavity as a function of time. This temperature is then used to determine the membrane position in order to couple the thermal model to the flow model.

Fig. 5 depicts the important structural parameters of the normally open microvalve, and relates them to the state variables (temperatures) used in the thermal model.

Using Fig. 5, the lumped element thermal model equations can be written (in state-variable format) to link the six temperature state variables (T_{py1}, T_{py2}, T_{FC}, $T_{\rm mem}$, T_{Si}, and $T_{\rm pkg}$), to the various structural and material parameters (w_b, t_{Si}, $t_{\rm mem}$, $t_{\rm cav}$, t_{py}, and a), and the boundary conditions ($T_{\rm res}$ and $T_{\rm amb}$). Thermal couplings between and among state variables and boundary conditions are shown as thermal resistances. Terms on the left-hand side of the equations represent thermal energy storage associated with the particular temperature state variable. Terms on the right-hand side of the equations represent thermal inputs to or outputs from the mass associated with the particular state variable. These thermal inputs or outputs can be due to

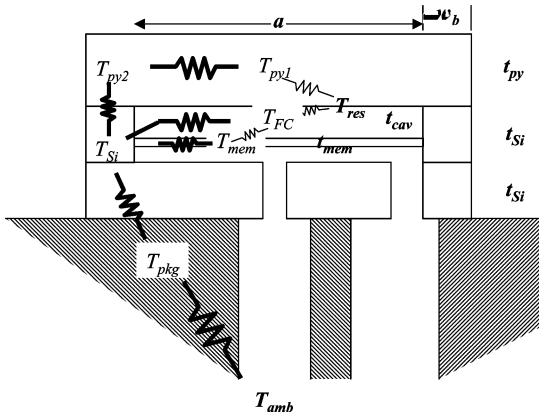

Fig. 5. Schematic of the normally open thermopneumatic microvalve structure depicting the lumped elements of the thermal model.

radiation or convection, but are primarily due to conduction. The state variables are implicitly time dependent. Boundary conditions which can also vary with time are indicated using the explicit time variable

$$\begin{aligned}
m_{py1}C_{py}\frac{dT_{py1}}{dt} &= \frac{T_{\rm res}(t)-T_{py1}}{R_{py1}} \\
&\quad - \frac{T_{py1}-T_{py2}}{R_{py2}} - \text{radiation} \\
m_{py2}C_{py}\frac{dT_{py2}}{dt} &= \frac{T_{py1}-T_{py2}}{R_{py2}} - \frac{T_{py2}-T_{Si}}{R_{py3}} \\
m_{FC}C_{FC}\frac{dT_{FC}}{dt} &= \frac{T_{\rm res}(t)-T_{FC}}{R_{FC1}} \\
&\quad - \frac{T_{FC}-T_{\rm mem}}{R_{FC1}} - \frac{T_{FC}-T_{Si}}{R_{FC2}} \\
m_{\rm mem}C_{Si}\frac{dT_{\rm mem}}{dt} &= \frac{T_{FC}-T_{\rm mem}}{R_{FC1}} - \frac{T_{\rm mem}-T_{Si}}{R_{\rm mem}} \\
&\quad - h_{\rm conv}(T_{\rm mem}-T_{\rm pkg}) \\
m_{Si}C_{Si}\frac{dT_{Si}}{dt} &= \frac{T_{py2}-T_{Si}}{R_{py3}} + \frac{T_{\rm mem}-T_{Si}}{R_{\rm mem}} \\
&\quad + \frac{T_{FC}-T_{Si}}{R_{FC2}} - \frac{T_{Si}-T_{\rm pkg}}{R_{Si}} \\
m_{\rm pkg}C_{\rm pkg}\frac{dT_{\rm pkg}}{dt} &= \frac{T_{Si}-T_{\rm pkg}}{R_{Si}} - \frac{T_{\rm pkg}-T_{\rm amb}(t)}{R_{\rm pkg}}. \qquad (17)
\end{aligned}$$

Overall, there are six state variables, which describe the thermal system. Among these is the cavity liquid temperature, which couples the thermal system to the mechanical portion of the structure. The first equation has allowance for radiative heat transfer off the top of the microvalve. The fourth equation shows the convective heat transfer, coupling the microvalve membrane and the package. Active power input is made using the platinum heater resistor temperature $T_{\rm res}(t)$.

This set of equations is valid for situations where power is applied actively to the microvalve. A modified set of equations must be used when the input power is zero, corresponding to cooling of the valve. These equations are

$$\begin{aligned}
m_{py1}C_{py}\frac{dT_{py1}}{dt} &= -\frac{T_{py1}-T_{FC}}{R_{py1}+R_{FC1}} \\
&\quad - \frac{T_{py1}-T_{py2}}{R_{py2}} - \text{radiation} \\
m_{py2}C_{py}\frac{dT_{py2}}{dt} &= \frac{T_{py1}-T_{py2}}{R_{py2}} - \frac{T_{py2}-T_{Si}}{R_{py3}} \\
m_{FC}C_{FC}\frac{dT_{FC}}{dt} &= \frac{T_{py1}-T_{FC}}{R_{py1}+R_{FC1}} \\
&\quad - \frac{T_{FC}-T_{\rm mem}}{R_{FC1}} - \frac{T_{FC}-T_{Si}}{R_{FC2}} \\
m_{\rm mem}C_{Si}\frac{dT_{\rm mem}}{dt} &= \frac{T_{FC}-T_{\rm mem}}{R_{FC1}} - \frac{T_{\rm mem}-T_{Si}}{R_{\rm mem}} \\
&\quad - h_{\rm conv}(T_{\rm mem}-T_{\rm pkg}) \\
m_{Si}C_{Si}\frac{dT_{Si}}{dt} &= \frac{T_{py2}-T_{Si}}{R_{py3}} + \frac{T_{\rm mem}-T_{Si}}{R_{\rm mem}} \\
&\quad + \frac{T_{FC}-T_{Si}}{R_{FC2}} - \frac{T_{Si}-T_{\rm pkg}}{R_{Si}} \\
m_{\rm pkg}C_{\rm pkg}\frac{dT_{\rm pkg}}{dt} &= \frac{T_{Si}-T_{\rm pkg}}{R_{Si}} - \frac{T_{\rm pkg}-T_{\rm amb}(t)}{R_{\rm pkg}}. \qquad (18)
\end{aligned}$$

In steady-state, without radiation or convection, a matrix equation can be solved to find the state variables. Radiation and convection add nonlinearities which do not lend themselves to matrix solution. Nonetheless, a matrix solution is useful when identifying initial or final values of the system state variables. This matrix (19), as shown at the bottom of the page, holds.

$$\begin{pmatrix}
\frac{1}{R_{py1}}+\frac{1}{R_{py2}} & -\frac{1}{R_{py2}} & 0 & 0 & 0 & 0 \\
\frac{1}{R_{py2}} & -\frac{1}{R_{py2}}-\frac{1}{R_{py3}} & 0 & 0 & \frac{1}{R_{py3}} & 0 \\
0 & 0 & \frac{2}{R_{FC1}}+\frac{1}{R_{FC2}} & -\frac{1}{R_{FC1}} & -\frac{1}{R_{FC2}} & 0 \\
0 & 0 & \frac{1}{R_{FC1}} & -\frac{1}{R_{FC1}}-\frac{1}{R_{\rm mem}} & \frac{1}{R_{\rm mem}} & 0 \\
0 & \frac{1}{R_{py3}} & \frac{1}{R_{FC2}} & \frac{1}{R_{\rm mem}} & -\frac{1}{R_{py3}}-\frac{1}{R_{FC2}}-\frac{1}{R_{\rm mem}}-\frac{1}{R_{Si}} & \frac{1}{R_{Si}} \\
0 & 0 & 0 & 0 & -\frac{1}{R_{Si}} & \frac{1}{R_{Si}}+\frac{1}{R_{\rm pkg}}
\end{pmatrix}$$

$$\times \begin{pmatrix} T_{py1} \\ T_{py2} \\ T_{FC} \\ T_{\rm mem} \\ T_{Si} \\ T_{\rm pkg} \end{pmatrix} = \begin{pmatrix} \frac{T_{\rm res}}{R_{py1}} \\ 0 \\ \frac{T_{\rm res}}{R_{FC1}} \\ 0 \\ 0 \\ \frac{T_{\rm amb}}{R_{\rm pkg}} \end{pmatrix}. \qquad (19)$$

The actual platinum resistor temperature is related to the measured power input, using physical measurement of the temperature-versus-resistance characteristic of the platinum resistor. For the model, this relationship is cast as an effective thermal resistance R_{th} as in

$$T_{\rm res}(t) = T_{\rm amb} + \text{Power}(t) \cdot R_{th}. \tag{20}$$

The linear nature of the problem allows this relationship to be used. From the model perspective, R_{th} is the overall thermal resistance between the heater resistor and the ambient temperature boundary condition.

Due to its highly distributed (i.e., nonlumped) nature, there is a perceptible time delay of perhaps 0.1 s between the instantaneous change in electrical power applied to the platinum resistor, and the actual change in the platinum resistor's temperature, as determined by its electrical resistance. To account for this observed behavior, the following can be used:

$$T_{\rm res}(t) = T_{\rm res,init} \exp\left(-\frac{t}{\tau_{\rm heater}}\right) + T_{\rm res,final}\left(1 - \exp\left(-\frac{t}{\tau_{\rm heater}}\right)\right). \tag{21}$$

The values of the various lumped thermal resistances in (17) and (18) can be gathered from Fig. 5. They use the defined distances in the structure as well as the material properties (density, thermal conductivity) of the structural components. Typically, in our microvalves, Pyrex and silicon are the principal materials, as suggested by the subscripts used in the lumped element parameters. Equation (22) defines the parameters

$$\begin{aligned}
m_{py1} &= \rho_{py} a^2 t_{py} \\
m_{py2} &= 4\rho_{py} t_{py} w_b (a + w_b) \\
m_{FC} &= \rho_{FC} a^2 t_{\rm cav} \\
m_{\rm mem} &= \rho_{Si} a^2 t_{\rm mem} \\
m_{Si} &= 4\rho_{Si} t_{Si} w_b (a + w_b) + \rho_{Si} t_{Si} (a + 2w_b)^2 \\
m_{\rm pkg} &= \rho_{\rm pkg} V_{\rm pkg} \\
R_{py1} &= \frac{\frac{t_{py}}{2}}{\kappa_{py} a^2} \\
R_{py2} &= \frac{\frac{a}{2}}{\kappa_{py} 4 t_{py} a} \\
R_{py3} &= \frac{\frac{t_{py}}{2}}{\kappa_{py} 4 w_b a} + \frac{\frac{t_{Si}}{2}}{\kappa_{Si} 4 w_b a} \\
R_{FC1} &= \frac{\frac{t_{\rm cav}}{2}}{\kappa_{FC} a^2} \\
R_{FC2} &= \frac{\frac{a}{2}}{\kappa_{FC} 4 t_{\rm cav} a} \\
R_{\rm mem} &= \frac{\frac{a}{2}}{\kappa_{Si} 4 t_{\rm mem} a} \\
R_{Si} &= \frac{\frac{t_{Si}}{2}}{\kappa_{Si} 4 w_b a} + \frac{t_{Si}}{\kappa_{Si} 4 w_b a} \\
R_{\rm pkg} &= \text{measured value.}
\end{aligned} \tag{22}$$

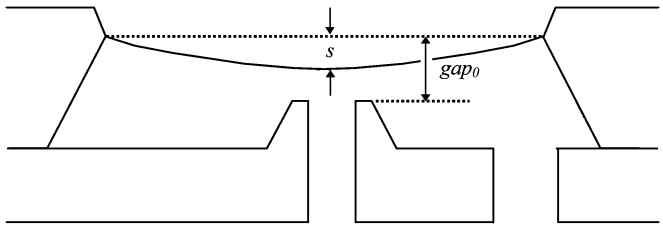

Fig. 6. Schematic of the normally open thermopneumatic microvalve structure, depicting the parameters which couple the thermal model to the flow model.

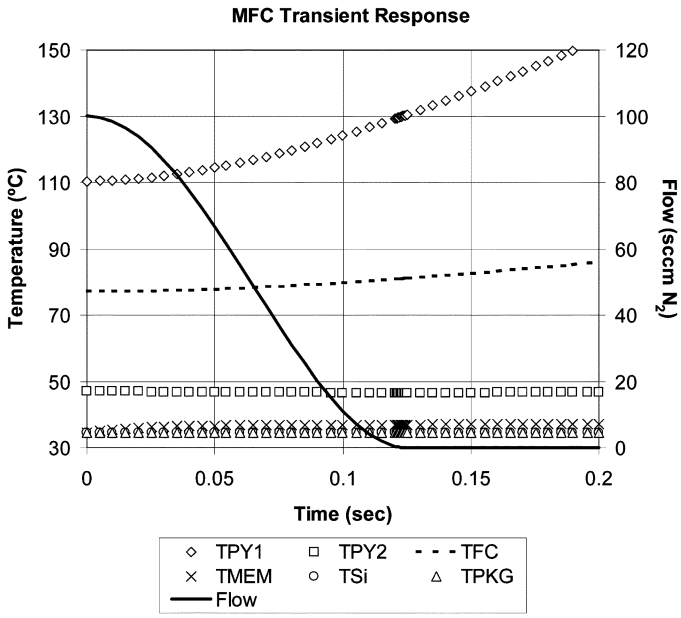

Fig. 7. Transient response of the temperature state variables and the simulated flow for a mass flow controller.

Given boundary conditions on $T_{\rm res}$ and $T_{\rm amb}$, the preceding systems of equations can be integrated forward in time using either Euler or Runge–Kutta techniques. The result of this procedure is the generation of the time-dependent behavior of all state variables. Note that, since the valve is rectangular, four-fold symmetry considerations are used to simplify the overall expression of the heat capacities and thermal resistivities.

With the mechanical displacement of the membrane now related to the mean Fluorinert temperature, we can relate the membrane position to the valve flow, coupling the mechanical and thermal models. Fig. 6 defines several required parameters.

Using Fig. 6, the following relationship is evident:

$$\text{gap}(s) = \text{Max}(0, \text{gap}_0 - s). \tag{23}$$

The quantitative flow relationships remain as those given in (14).

The full transient model has been characterized in a number of ways. Several aspects will be presented as follows.

Fig. 7 shows an example of the simulated transient response of a normally open microvalve used as a mass flow control valve. Table I shows the valve structural and material parameters used in the model; the model size/structural parameters are taken directly from the actual valve studied. The initial power to the

TABLE I
VALUES OF MODEL PARAMETERS USED IN THE SIMULATION RESULTS SHOWN IN FIGS. 7–10

ρ_{Py}	2230	a	0.0045
ρ_{Si}	2328	w_b	0.001
$\rho_{Fluorinert}$	1680	t_{cav}	0.0004
ρ_{pkg}	7760	t_{Si}	5.00E-04
C_{Py}	754	package side	0.03
C_{Si}	890	t_{pkg}	0.0075
$C_{Fluorinert}$	1050	package length	0.03
C_{pkg} (Alloy 42)	490	t_{Py}	800e-6
κ_{Py}	1.21	$t_{membrane}$	50e-6
$\kappa_{Fluorinert}$	0.06	gap_0	20e-6
κ_{Si}	149		
κ_{pkg}	13		

valve is 1.485 W. At $t = 0$, 5 W of power is applied to the valve. The state variables and the flow respond as shown in Fig. 7. The simulated response time is extracted and compared to the measured response time.

Extending this example, we next compare the modeled and measured flow response times for the normally open microvalve, going from an open condition to a closed condition, as in Fig. 7. The variable in this study is the maximum power applied to the platinum heater resistor. Fig. 8 shows the comparison between the measured and modeled results.

The second example compares the modeled and measured flow response times for the normally open microvalve, going from a closed position to an open condition. In this instance, however, no active power is applied to the valve. Instead, the response time is measured and modeled as a function of variations in the thickness of the Pyrex layer in the microvalve. Fig. 9 shows the results. The observation of a decrease in response time for thicker Pyrex was unexpected: The heat capacity of the added mass and its ability to transfer excess heat into the thermopneumatic fluid cavity, thereby slowing the cool-down process, was thought to be the dominant effect. Instead, as the measurements showed and the model confirmed, the reduction in thermal resistance afforded by the thicker Pyrex resulted in shorter response times for thicker Pyrex.

VI. DISCUSSION

The membrane center deflection is a nonlinear function of the change in hermetic cavity volume, as seen through the combination of (1) and (2). However, in some of the actual analysis performed in this work—specifically, in the transient analysis of a normally-open valve, presented previously—a linear relationship was presumed. Changing to a more complete description of the membrane deflection affects the results slightly, but does not compromise the overall success of the model, relative to actual measurements. It was also mentioned in Section II that η_V may not be a constant of the center deflection s. For the normally open valve studied in Section V, the value of η_V changes from 0.346 for $s = 0$ to a value of 0.394 for $s = 84$ μm. Again, the change imparted on the overall model of this additional complexity is modest at worst and negligible at best.

In coupling the membrane mechanical model to the normally open microvalve flow model, the membrane is taken to be essentially flat at the point of contact with the valve seat, so that the gap between membrane and valve seat closes uniformly, in a simple manner. In fact, the percentage of the valve seat area covered by the membrane has a complex behavior. The use of membranes with a central boss, to ensure a flat aspect between the membrane and the valve seat, can overcome this complexity. On the other hand, a membrane without a boss can, through its flexibility across the span of the membrane, provide benefits in closure and control. This advantage is particularly true if the valve seat has a more complicated aspect, as in multiple holes, or a convoluted perimeter profile [20], [22]: Central portions of the valve seat structure will be sealed first, while outer portions of the valve seat will only be sealed after additional deflection of the membrane away from the center.

The thermopneumatic cavity is assumed to be isobaric under the fill conditions, and again under any other conditions of inlet pressure and ambient temperature. This assumption holds well. The cavity is also assumed to be isobaric under nonequilibrium (but steady-state) thermal conditions: That is, if a thermal gradient exists through the hermetic cavity and its fluid constituents. This assumption is also accurate, but there are complications [7]. In particular, if both liquid and vapor phases exist in it, the pressure of the cavity will be set entirely by the mean temperature at the interface between the liquid and vapor phases. Clearly, nonequilibrium conditions (and transient conditions as well) will complicate the detailed model of the hermetic cavity. Boiling, for instance, means that a clear interface between the two phases does not exist. For the thermopneumatic microvalves in this study, boiling can be observed in the transition from an all-liquid state, to a liquid-vapor state. However, this transition usually occurs quickly, and the boiling is observed (directly, through the Pyrex portion of the structure) to subside quickly, resulting in the achievement of a clear interface between liquid and vapor phases. In the case of microvalves controlling the flow of a gas, the presence of boiling can also be observed indirectly: boiling in the thermopneumatic cavity results in a "flutter" of the membrane, which causes increased noise in the measured gas flow through the device.

An additional complication which can occur is related to the Fluorinert materials chosen as the thermopneumatic fluid in the actuator cavities studied here. That is, Fluorinert can, to a high degree, absorb substantial amounts of gas, especially carbon dioxide [17]. For actuators where the control fluid moves back and forth between liquid-only and liquid-vapor states, the dynamics of the transition can be complicated by the presence of these absorbed gases. Care must be taken, therefore, to control the concentrations of such gases, during the process of incorporating the Fluorinert fluids into the hermetic thermopneumatic cavity.

Lumped element models have been taken to describe the conduction of heat throughout the valve structures modeled in this paper, except for the highly distributed platinum resistor associated with the thermopneumatic cavity heater. The success of the model against measured structures validates the lumped element approach, and implies that, on the time scale of the transient phenomena studied here, the thermal character of the microvalve structures can be considered to be quasi-steady-state, so that ordinary differential equations [such as (17)] can be used to describe the time dependence of the system, without requiring

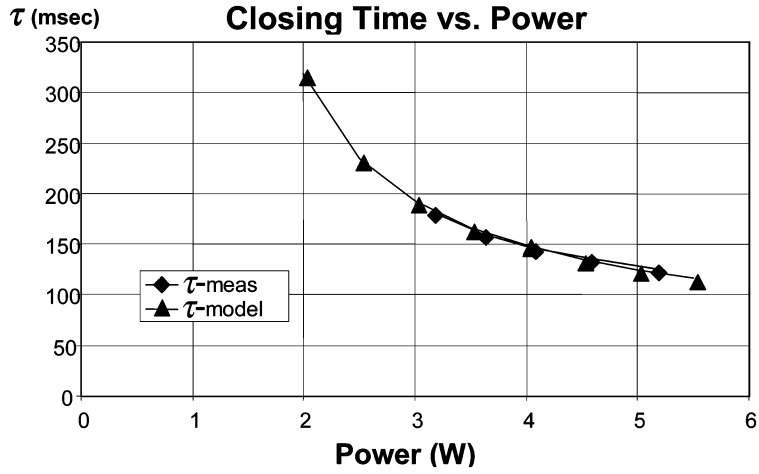

Fig. 8. Comparison of the measured and modeled closing times for flow through a mass flow controller, comprised of a normally open thermopneumatic microvalve and a flow sensor [21].

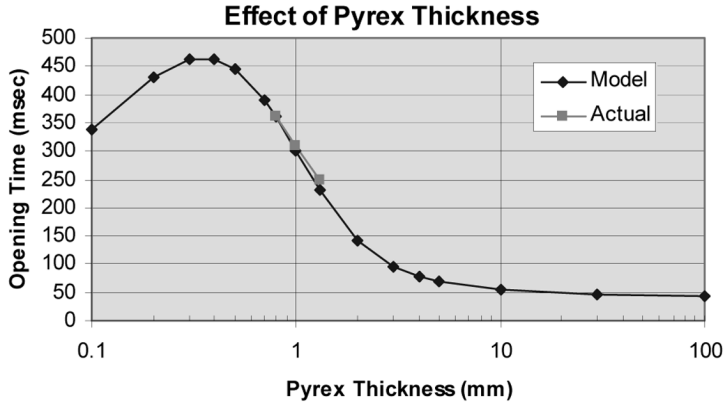

Fig. 9. Comparison of the measured and modeled opening times for flow through a mass flow controller, comprised of a normally open thermopneumatic microvalve and a flow sensor, versus the thickness t_{py} of the Pyrex layer in the microvalve (see Fig. 5).

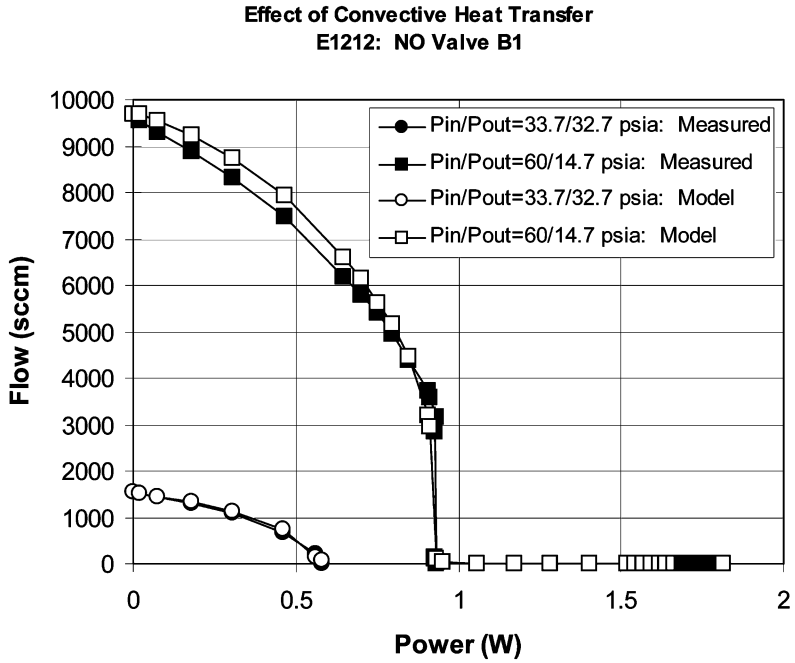

Fig. 10. Effect of including convective heat transfer in a normally open microvalve with thermopneumatic actuation. Inlet and outlet pressures (psia) are given in the legend. The equilibrium gap is 30 μm, and the inlet port is 1500 μm square. The Fluorinert is FC-43, with a fill temperature of 70 °C. The coefficient of discharge is 0.76, and the ambient temperature is 25 °C.

a full partial differential equation approach, or finite-element analysis. The platinum heater is approximately 1-μm-thick, and has a room-temperature resistance of approximately 50 Ω. The width is approximately 200 μm.

In the present treatment, heat loss via radiation through the top of the normally open valve in the transient response case has been ignored, particularly in the solution of (17). The validity of this treatment can be considered as follows. The radiative power loss is given by

$$P_{\rm rad} = \varepsilon \sigma_{SB} A_{\rm rad} \left(T_{py1}^4 - T_{\rm amb}^4 \right). \tag{24}$$

If the emissivity for the Pyrex is taken as unity (a very conservative assumption), then using a radiative area of 6.3 mm, and Pyrex and ambient temperatures of, respectively, 117 °C and 25 °C, the radiative power loss is only about 34 mW. Obviously, larger values of the Pyrex temperature would demand inclusion of this heat loss mode, but for the valves considered herein, neglect of this mode does not compromise the performance of the model.

Heat loss via convection, through interaction with the controlled gas, is included in the normally open valve model represented by (17). In characterizing the model, by measuring and modeling steady-state flow versus power, for normally open valves of the type studied here, the convective heat transfer coefficient becomes important when, for nitrogen, gas flow rates exceed roughly 200 sccm. Below this flow rate, there is no substantial contribution to the thermal behavior of the microvalve from convective heat transfer. Fig. 10 shows how microvalves with higher flow rates can be affected. The figure caption gives the particulars of the microvalve structural parameters and boundary conditions for flow. Other parameters not specified are identical to those in Table I. From this characteristic, it was determined that the convective heat transfer coefficient has the following behavior with respect to flow:

$$h_{\rm conv} = 10^{-4} \sqrt{\dot{m}}. \tag{25}$$

In this formulation, the flow rate has units of sccm. Note that, unlike the usual form for convective heat transfer, the effective area for convective heat transfer is incorporated into $h_{\rm conv}$. As a consequence, this parameter must be considered unique to the particular microvalve structure. Extension to alternative structures requires more substantial characterization.

Also, in the normally open valve example, the Fluorinert is assumed to completely fill the cavity. That is, the fill factor η_f is unity. The effect of this parameter on actual devices has not been studied.

VII. Conclusion

A comprehensive model for thermopneumatic actuators has been developed. It has been applied to thermopneumatic microvalves and characterized under steady-state and transient conditions. The full thermodynamic state of the working fluid is incorporated in the model. The storage and transport of thermal energy is handled by using lumped thermal storage and dissipative elements (thermal capacitors and resistors). The effect on the actuator of convective cooling due to microvalve gas flow has also been included. The model provides a powerful tool for the design of all such actuators, for any working fluid used in the actuator, for any actuator structure, and for any set of boundary conditions, provided one is willing to exert a bit of effort to create lumped thermal models for the various thermal capacitors and resistors in the actuator.

Acknowledgment

The author would like to thank M. Zdeblick whose early work on thermopneumatic actuation, and the author's early collaborations with him, laid important foundations for this work. He would also like to thank a number of co-workers at Redwood Microsystems, particularly with J. Harris, D. Hopkins, B. Cozad, M. Selser, J. Fitch, E. Lawrence, S. Patel, J. Hill, and H. Dinh, for their collaboration concerning the fabrication and characterization of some of the devices reported herein. A fruitful collaboration with A. Zias on silicon membrane pressure sensors provided insight regarding the behavior of membranes, which is important to this work.

References

[1] M. J. Zdeblick and J. B. Angell, "A microminiature electric-to-fluidic valve," in *Proc. Transducers '87*, 1987, pp. 827–830.

[2] M. Zdeblick, "A planar process for an electric-to-fluidic valve," Ph.D. dissertation, Dept. Elect. Eng., Stanford Univ., Stanford, CA, 1988.

[3] ——, "Integrated, microminiature electric-to-fluidic valve and pressure/flow regulator," U.S. Patent 4 821 997, 1989.

[4] M. J. Zdeblick, R. Anderson, H. Jankowski, B. Kline-Schroeder, L. Christel, R. Miles, and W. Weber, "Thermopneumatically-actuated microvalves and integrated electro-fluidic circuits," in *Proc. Solid-State Sens. Actuator Workshop*, 1994, pp. 251–254.

[5] P. L. Bergstrom, J. Ji, Y.-N. Liu, M. Kaviany, and K. D. Wise, "Thermally driven phase-change microactuation," *J. Microelectromech. Syst.*, vol. 4, no. 1, pp. 10–17, Mar. 1995.

[6] B. A. Cozad, "Apparatus and method for controlling fluid in a micromachined boiler," U.S. Patent 6 160 243, 2000.

[7] A. K. Henning, "Liquid and gas-liquid phase behavior in thermopneumatically actuated microvalves," in *Proc. Micro Fluidic Devices Syst., SPIE.*, 1998, vol. 3515, pp. 53–63.

[8] A. K. Henning, J. Fitch, E. Falsken, D. Hopkins, L. Lilly, R. Faeth, and M. Zdeblick, "A thermopneumatically actuated microvalve for liquid expansion and proportional control," in *Proc. Transducers '97: Int. Solid State Sensors Actuators Conf.*, 1997, pp. 825–828.

[9] A. K. Henning, M. Zdeblick, J. S. Fitch, D. A. Hopkins Jr, and L. J. Lilly, "Low-power thermopneumatic microvalve," U.S. Patent 6 129 331, 2000.

[10] X. Yang, C. Grosjean, Y.-C. Tai, and C.-M. Ho, "A MEMS thermopneumatic silicone membrane valve," in *Proc. IEEE 10th Annu. Int. Workshop Microelectromech. Syst. (MEMS '97)*, 1997, pp. 114–118.

[11] Y.-C. Tai, X. Yang, C. Grosjean, and X.-Q. Wang, "Micromachined parylene membrane valve and pump," U. S. Patent 6 345 502, 2002.

[12] E. T. Carlen and C. H. Mastrangelo, "Surface micromachined paraffin-actuated microvalve," *J. Microelectromech. Syst.*, vol. 11, no. 5, pp. 408–420, Oct. 2002.

[13] C. A. Rich and K. D. Wise, "A high-flow thermopneumatic microvalve with improved efficiency and integrated state sensing," *J. Microelectromech. Syst.*, vol. 12, no. 2, pp. 201–208, Apr. 2003.

[14] M. M. Athavale, H. Q. Yang, and A. J. Przekwas, "Coupled fluid-thermal-structural simulations in microvalves and microchannels," in *Proc. Int. Conf. Modeling Simulation Microsyst. (MSM'99)*, 1999, pp. 570–573.

[15] M. D. Giovanni, *Flat and Corrugated Diaphragm Design Handbook*. New York: Marcel Dekker, 1982, p. 130ff.

[16] L. E. Andreeva, *Elastic Elements of Instruments*. Jerusalem: Israel Program for Scientific Translations, 1962, p. 196ff.

[17] *Fluorinert™ Electronic Liquids Product Manual*. St. Paul, MN: 3M Corp., 1987.

[18] O. Redlich and J. N. S. Kwong, "On the thermodynamics of solutions V: An equation of state. Fugacities of gaseous solutions," *Chem. Rev.*, vol. 44, pp. 233–244, 1949.

[19] J. M. Harris, J. S. Fitch, B. A. Cozad, and D. A. Hopkins Jr, "Integrated electrically operable normally closed valve," U.S. Patent 5 865 417, 1999.

[20] A. K. Henning, "Improved gas flow model for microvalves," in *Proc. Transducers 2003: Int. Solid State Sensors Actuators Conf.*, 2003, pp. 1550–1553.
[21] A. K. Henning, J. S. Fitch, J. M. Harris, E. B. Dehan, B. A. Cozad, L. Christel, Y. Fathi, D. A. Hopkins, Jr, L. J. Lilly, W. McCulley, W. A. Weber, and M. Zdeblick, "Microfluidic mems for semiconductor processing," *IEEE Trans. Compon., Packag., Manuf. Technol. B*, vol. 21, no. 4, pp. 329–337, Nov. 1998.
[22] A. K. Henning, M. Selser, and B. A. Cozad, "High-flow microvalve," U.S. Patent 6 986 365, 2006.

Albert K. Henning (M'79) received the A.B. and A.M. degrees in physics from Dartmouth College, Hanover, NH, in 1977 and 1979, respectively, and the Ph.D. degree in electrical engineering from Stanford University, Stanford, CA, in 1987, studying hot carrier metal–oxide–semiconductor field-effect transistor (MOSFET) physics at cryogenic temperatures.

From 1979 to 1982, he was a Device Physicist with Intel Corporation, where he led the initial complimentary metal–oxide–semiconductor (CMOS) device physics analysis, and developed transistor designs for the 386 generation of microprocessors. From 1987 to 1995, he was Assistant and Associate Professor of Engineering Science at Dartmouth College, working on semiconductor device physics (including hot carrier effects and MEMS-based scanning probe metrology of MOSFET doping profiles and defects), and beginning his research into microflow devices, such as microscale flow channels, scaled inkjet orifices, and microvalves and microturbines. Beyond his funded research projects at Dartmouth, he developed two National Science Foundation (NSF)-sponsored projects, an undergraduate course on MEMS, and a summer workshop on MEMS for minority students. In 1996, he joined Redwood Microsystems, where he was Director of Technology until Redwood's closure in 2006. In conjunction with SemiZone, Palo Alto, CA, he developed a distance learning course on microflow devices. He has published over 60 journal articles and proceedings papers and holds six U.S. patents. His research interests concern the physics and technology of microflow structures and systems, particularly with respect to valves, orifices, and pressure sensors. Application interests have included increased refrigeration efficiency using microvalves; high-performance, high-reliability mass flow control using microflow components; advanced microscale pressure sensors; precision liquid metering; novel microactuator technologies; and integrated microflow systems for applications including microfuel cells.

Dr. Henning is active in the IEEE and the MEMS-related SPIE conferences. He was the holder of an Analog Devices Career Development Professorship, and an IBM Faculty Development Award.